Efficacy of Electrical Stimulation of Retinal Ganglion Cells with Temporal Patterns Resembling Light-Evoked Spike Trains

Raymond C. S. Wong, David J. Garrett, David B. Grayden,
Michael R. Ibbotson and Shaun L. Cloherty

***Abstract*— People with degenerative retinal diseases such as retinitis pigmentosa lose most of their photoreceptors but retain a significant proportion ($\sim$30%) of their retinal ganglion cells (RGCs). Microelectronic retinal prostheses aim to bypass the lost photoreceptors and restore vision by directly stimulating the surviving RGCs. Here we investigate the extent to which electrical stimulation of RGCs can evoke neural spike trains with statistics resembling those of normal visually-evoked responses. Whole-cell patch clamp recordings were made from individual cat RGCs *in vitro*. We first recorded the responses of each cell to short sequences of visual stimulation. These responses were converted to trains of electrical stimulation that we then presented to the same cell via an epiretinal stimulating electrode. We then quantified the efficacy of the electrical stimuli and the latency of the evoked spikes. In all cases, spikes were evoked with sub-millisecond latency ($0.55\,\mathrm{ms}$, median, ON cells, $n = 8$; $0.75\,\mathrm{ms}$, median, OFF cells, $n = 6$) and efficacy ranged from 0.4-1.0 (0.79, median, ON cells; 0.97, median, OFF cells). These data demonstrate that meaningful spike trains, resembling normal responses of RGCs to visual stimulation, can be reliably evoked by epiretinal prostheses.**

I. Introduction

MICROELECTRONIC retinal prostheses aim to restore the sense of sight to individuals suffering degenerative disease of the retina. These devices target the surviving retinal ganglion cells (RGCs) that form the output of the retina and convey visual signals to the brain. Given that RGCs can fire at high rates ($>$ 200 spikes per second) in response to normal visual stimulation, the ability to evoke high firing rates in RGCs in response to prosthetic stimulation is of direct consequence to the development of functional retinal prostheses. However, reports on the response of RGCs to repetitive stimulation, particularly at high frequencies, have been mixed [1]–[4].

In most studies to date, electrical stimuli consisted of trains of electrical stimulus pulses delivered at a fixed frequency. Such stimuli do not resemble the statistics of RGC spike trains evoked by normal visual stimuli, which typically exhibit highly reliable temporal structure. Fried *et al.* [1] directly investigated the ability of prosthetic stimulation to reproduce visual responses from rabbit RGCs. They reported that electrical stimulation was able to evoke spike trains from RGCs that precisely match those evoked by presentation of a simple visual stimulus. However, the data supporting this assertion is extremely limited – they show results for only a single RGC of unknown type.

Here we investigate the extent to which electrical stimulation can evoke spiking responses from RGCs, with statistics resembling those of normal visual responses. We made *in vitro* patch-clamp recordings of responses to both visual and electrical stimulation from ON- and OFF-center brisk-transient (BT) RGCs in normal cat retina. We found that biphasic current pulses typically evoked a single action potential with sub-millisecond latency ($0.55\,\mathrm{ms}$, median, ON-BT cells; $0.75\,\mathrm{ms}$, median, OFF-BT cells; $0.65\,\mathrm{ms}$, median, all cells). Notably, we add to previous reports by quantifying the efficacy of electrical stimulation in both ON- and OFF-BT RGCs. We found that the efficacy of electrical stimulation resembling light-evoked responses was high for most cells (0.79, median, ON-BT cells, $n = 8$; 0.97, median, OFF-BT cells, $n = 6$; 0.92, median, all cells).

II. Methods

All experimental procedures were performed in strict compliance with the Australian Code of Practice for the Care and Use of Animals for Scientific Purposes from the National Health and Medical Research Council of Australia, and were approved by the Animal Experimentation Ethics Committee of the Faculty of Science, University of Melbourne.

A. Retinal Wholemount Preparation

Experiments were performed on the retinas of 8 normally sighted cats of both sexes ranging in age from 4 to 24 months (1.5-$3.0\,\mathrm{kg}$). Animals were anesthetized by i.m. injection of a mixture of Ketamine ($20\,\mathrm{mg.kg^{-1}}$) and Xylazine ($1\,\mathrm{mg.kg^{-1}}$). Once deeply anaesthetised, both eyes were enucleated and the animals immediately killed by intracardiac injection of sodium pentobarbitone ($150\,\mathrm{mg.kg^{-1}}$). The eyes were immersed into Ames solution (Ames' medium,

This research was supported by the Australian Research Council through its Special Research Initiative in Bionic Vision Science and Technology grant to Bionic Vision Australia (BVA), and by the National Health and Medical Research Council of Australia through Project grant 585440. The Bionics Institute acknowledges the support it receives from the Victorian Government through its Operational Infrastructure Support Program.

R. C. S. Wong, National Vision Research Institute, Australian College of Optometry, VIC 3053; Research School of Biology, Australian National University, ACT 2601, Australia.

D. J. Garrett, Bionics Institute, 384-388 Albert Street, VIC 3002, Australia.

D. B. Grayden, NeuroEngineering Laboratory, Department of Electrical and Electronic Engineering, University of Melbourne, VIC 3010; Centre for Neural Engineering, University of Melbourne, VIC 3010; Bionics Institute, 384-388 Albert Street, VIC 3002, Australia.

M. R. Ibbotson, National Vision Research Institute, Australian College of Optometry, VIC 3053; ARC Centre of Excellence for Integrative Brain Function; Department of Optometry and Vision Sciences, University of Melbourne, VIC 3010, Australia.

S. L. Cloherty, National Vision Research Institute, Australian College of Optometry, VIC 3053; Department of Electrical and Electronic Engineering, University of Melbourne, VIC 3010, Australia.

978-1-4244-7929-0/14/$26.00 ©2014 IEEE

$8.8\,\mathrm{g.L^{-1}}$, 23 mM $\mathrm{NaHCO_3}$, 10 mM D-Glucose; all Sigma-Aldrich) containing 1% Pen-strep Glutamine (GIBCO), 1% N2 supplement (GIBCO), 1% horse serum and 0.1% phenol-red and bubbled with carbogen (95% O_2 and 5% CO_2). The eyes were hemisected behind the ora serrate and the vitreous body was removed. We removed a section of retina containing the area centralis (apical angle of the sector was $\sim 60^\circ$). The sclera was removed keeping the pigment epithelium and choroid attached. The retinal piece was then mounted onto a cover slip, RGC side up. The slip with the retina on it formed the bottom of a perfusion chamber (RC-26GLP, Warner Instruments, Hamden, CT). The tissue was held in place with a stainless steel harp fitted with Lycra threads (SHD-25GH, Warner Instruments). The chamber was mounted on the stage of an upright microscope (BX51WI, Olympus) equipped with a 40x water immersion lens. The tissue was continuously superfused ($9\text{-}11\,\mathrm{mL.min^{-1}}$) with Ames solution equilibrated with carbogen, and kept under dim red illumination at $34 \pm 0.5^\circ\mathrm{C}$. Under these condition the retina remained viable for 12-16 hours.

B. Patch-clamp Recordings

Patch-clamp recordings were obtained as described previously [5][6]. In brief, a small hole was made in the inner limiting membrane and nerve fiber layer to expose the RGCs. Exposed RGCs were targeted for recording based on soma size (we targeted cells with soma sizes $>20\,\mu\mathrm{m}$) and appearance (only cells with smooth appearance and agranular cytoplasm were targeted). Recordings were made in the whole-cell configuration using patch pipettes with impedances of $4\text{-}5\,\mathrm{M\Omega}$, containing (in mM): K-gluconate 115, KCl 5, EGTA 5, HEPES 10, ATP-Na 2, GTP-Na 0.25 (mOsm = 282, pH = 7.3).Prior to recording, the pipette voltage in the bath was nulled. After patching a cell the pipette series resistance was compensated using the bridge balance circuit of the amplifier (BA-1S, NPI). No capacitance compensation was employed. Membrane potential was amplified and sampled at $40\,\mathrm{kHz}$ (USB-6221, National Instruments).

C. Visual Stimuli

Visual stimuli were presented by way of an OLED microdisplay (SVGA+ Series OLED-XL, eMagin Corp.) mounted on the camera port of the microscopes trinocular head. Images rendered on the display were projected back through the microscopes optics and focused on the photoreceptor layer of the retina. Visual stimuli were controlled by a computer and consisted of parametrically defined spots and gratings (for functional cell classification) and short sequences of naturalistic images.

Image sequences were generated as follows. A human observer wearing a head mounted camera and eye tracker (SMI iView X HED, SensoMotoric Instruments GmbH) was asked to freely view an outdoor scene (Fig. 1A). Images of the scene and corresponding eye position signals were sampled at $50\,\mathrm{Hz}$. The subject viewed the scene through the window of the laboratory such that the scene was outdoors and subject to the prevailing natural illumination, while the observer remained inside, with the camera and eye tracker tethered to the acquisition computer.

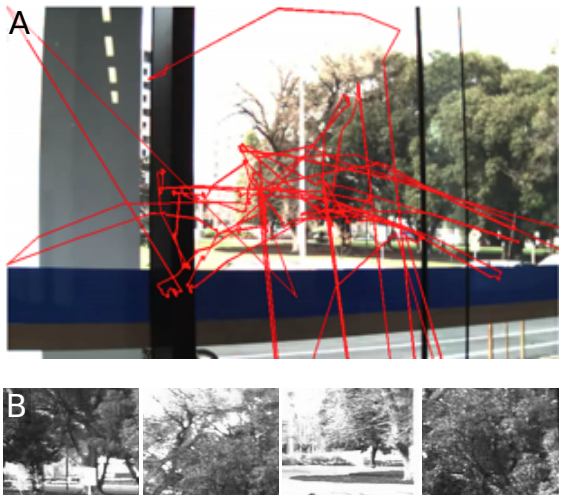

Fig. 1. Visual stimulus. A. A representative video frame showing the eye position of the observer over the duration of the raw video sequence overlayed in red. B. Example frames from the resulting stimulus sequence.

Stimulus sequences were then constructed by extracting from each raw video frame an image centred on the corresponding eye position vector. These images were landscape-oriented with an aspect ratio of 4:3 and an effective visual angle of $18.6^\circ \times 13.9^\circ$ when projected onto the retina (examples are shown in Fig. 1B).

D. Electrical Stimuli

Electrical stimuli were trains of asymmetric, charge-balanced, cathodic-first, biphasic current pulses ($100\,\mu\mathrm{s}$, cathodic phase; $400\,\mu\mathrm{s}$, anodic phase; $40\,\mu\mathrm{s}$ inter-phase interval). The amplitude of the biphasic waveform was adjusted for each cell (cathodic phase amplitude $1\,\mu\mathrm{A}\text{-}1\,\mathrm{mA}$) to ensure at least 90% efficacy for trains of 10 pulses delivered at $2\,\mathrm{Hz}$. Stimuli were produced by an electrical stimulator (STG4004-1.6mA, Multi Channel Systems GmbH) under software control and delivered to the target neuron via an epiretinal stimulating electrode, $200\,\mu\mathrm{m} \times 200\,\mu\mathrm{m}$ in size, fabricated from nitrogen doped ultra-nanocrystaline diamond (N-UNCD) [7]. Stimulating electrodes were placed approximately $50\,\mu\mathrm{m}$ from the cell soma, on top of the inner limiting membrane [5]. A return electrode was placed as close as was practical on the opposite side of the soma.

E. Data Analysis

We quantified the efficacy of our electrical stimuli as the proportion of stimulus pulses that evoked an action potential from the recorded cell. We further quantified the latency of the evoked responses. Both measures are readily derived from the cross-correlogram (CCG) of the evoked spike trains with the stimulus sequence [8]. To this end, the stimulus sequence and the spike trains were encoded as binary sequences with temporal resolution (Δt) of $0.1\,\mathrm{ms}$. We then calculated the CCG of the stimulus sequence ($s(t)$)

and the spike train from the i^{th} trial ($x_i(t)$) according to Bair *et al.* [9], i.e.,

$$CCG_i(\tau) = \frac{1}{\Delta t} \sum_{t=1}^{T} \frac{s(t)x_i(t+\tau)}{H(\tau)\sqrt{n_s n_i}} \quad (1)$$

where T is the duration of the sequences and $H(\tau)$ is a triangle function representing the extent of overlap of the two sequences at each value of τ, i.e.,

$$H(\tau) = T - |\tau|$$

We normalised by the geometric mean of the number of stimuli and the number of spikes (n_s and n_i, respectively) and by the bin width (Δt) in seconds. The units of our CCG are spikes per stimulus event. Efficacy is derived as the sum of the bins forming the main peak of the trial averaged CCG. The latency of the response is given by the position (τ) of the bin with the highest value.

III. Results

Here we report results from 14 brisk-transient (BT) RGCs (8 ON and 6 OFF) in normal cat retina. We based our cell classification entirely on the physiological responses to simple visual stimuli and, as such, we have referred to the cells as BT-RGCs. While we have refrained from giving the cells anatomical classifications, their physiology suggests that they are alpha cells [10].

Figure 2A shows an example membrane potential recording from a representative ON-BT cell during presentation of the 14 s visual stimulus. The movie elicited robust spiking responses from the cell interleaved by periods of hyperpolarisation. Figure 2B shows raster plots from 13 such recordings from the same cell. Figure 2C shows the peri-stimulus time histogram (PSTH) of the responses in Fig. 2B.

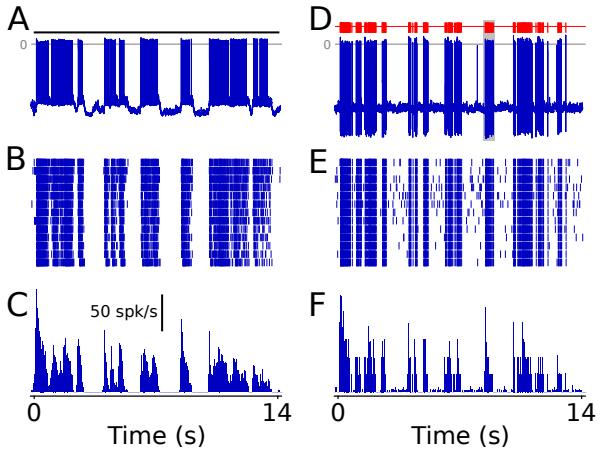

Fig. 2. Example responses to visual and electrical stimulation. A. An example membrane potential recording from an ON-BT RGC during presentation of the visual stimulus sequence (shown by the black bar). B. Raster plot showing spike times during repeated presentations of the visual stimulus. C. The peri-stimulus time histogram showing mean spike rate during presentation of the visual stimulus. D. An example membrane potential recording from the same example cell during presentation of the electrical stimulus sequence (shown in red). E. Raster plot showing responses to repeated presentation of the electrical stimulus. F. The peri-stimulus time histogram showing mean spike rate during presentation of the electrical stimulus.

Spiking responses were robust and reproducible. Based on the spiking responses of the cell to presentation of the visual stimulus, we constructed an electrical stimulus sequence (Fig. 2D; red) whose statistics resembled the light-evoked responses. We then presented this sequence to the cell by way of the epiretinal stimulating electrodes. Figure 2D shows a membrane potential recording from the example cell during presentation of this electrical stimulus sequence. Figures 2E and 2F show raster plots and the PSTH from 13 such recordings for comparison with the responses evoked by the visual stimulus (Figs. 2B and 2C). Responses to the electrical stimulus were robust and highly reproducible.

Figure 3A shows a segment of the recording in Fig. 2D (gray shaded region) with the time scale expanded to resolve individual stimulation events. This burst of stimulation contain several failed stimulation events (arrows in Fig. 3A), evident by the presence of the stimulus artefact but no subsequent action potential. Short segments of the membrane potential recording around each stimulation event are shown in Fig. 3B, aligned at the onset of each stimulus (gray traces show failed stimulation events). Figure 3C shows the same data after subtraction of the stimulus artefact (estimated by averaging the recorded waveform around the time of failed

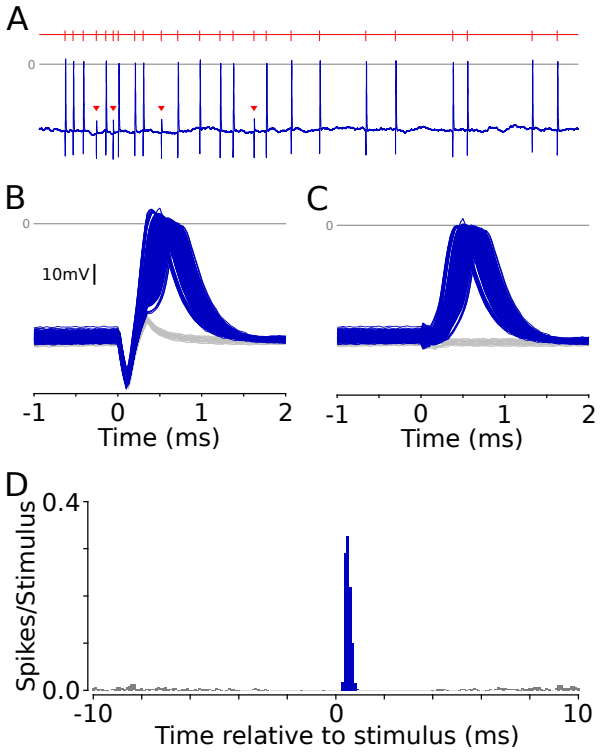

Fig. 3. Quantifying efficacy and spike latency for electrical stimulation. A. A 500 ms segment of the membrane potential recording shown in Fig. 2D (shaded region), scaled to illustrate successful and failed (arrows) stimulation events. B. Short segments of the membrane potential recording aligned at the onset of each electrical stimulus pulse. Successful stimulation events are shown in blue and failed stimulation events in grey. C. The same as in B after subtraction of the stimulus artefact to reveal the evoked action potential waveforms. The resulting action potential waveforms illustrate the range of spike latencies (i.e., 0-1.0 ms). D. The raw cross-correlogram (CCG), averaged across trials, showing efficacy and the distribution of spike latency across all trials.

stimulation events). Figure 3C reveals the range of spike latencies with respect to the electrical stimuli. In all cases, action potentials were evoked with sub-millisecond latency.

We quantified the efficacy of the electrical stimulation and the latency of the evoked action potentials by calculating the mean cross-correlogram function (CCG), averaged across trials, between the stimulus sequence and the recorded responses. Figure 3D shows the mean CCG for the example cell shown in Fig. 2. The efficacy of the electrical stimulus (i.e., the area under the main peak of the CCG; blue bars) for this cell was 0.98. The latency of evoked spikes (i.e., the location of the main peak of the CCG relative to stimulus onset) was $0.5\,\mathrm{ms}$.

Figure 4A compares the distribution of stimulus efficacy for the two groups of cells. The median efficacy was lower for electrical stimulation of ON-BT cells (0.79 for ON vs 0.97 for OFF). However, this difference was not significant (Kruskal-Wallis, $p = 0.27$). Figure 4B compares the distribution of spike latency for the two groups of cells. We found no significant difference in spike latency for the two cell groups ($0.55\,\mathrm{ms}$ for ON vs $0.75\,\mathrm{ms}$ for OFF; Kruskal-Wallis, $p = 0.29$).

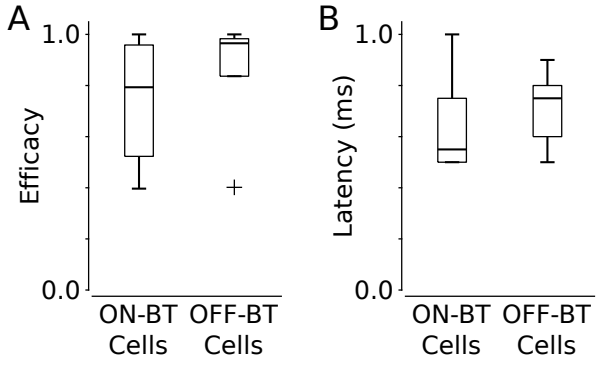

Fig. 4. Population data. A. Comparison of stimulus efficacy for ON- and OFF-BT RGCs. B. Comparison of spike latency for ON- and OFF-BT RGCs. In A and B the horizontal lines indicate the medians of the distributions, the rectangles indicate the inter-quartile range and the whiskers encapsulate the remainder of the data. Outliers are indicated by '+' symbols.

IV. Discussion

The novelty of our paradigm compared to previous studies is that we generated stimulus pulse trains that resembled the spiking responses of the recorded cells to visual stimuli. Moreover, our visual stimuli were derived from a sequence of eye movements recorded while freely viewing a natural scene. They therefore resemble the visual input to RGCs during normal vision, wherein periods of fixation are interspersed by saccadic eye movements [11]. The responses evoked by the visual stimuli and, as a result, the temporal patterns of electrical stimulation were sporadic in nature, unlike the regular periodic stimuli more typically used [1]–[4]. Our experimental paradigm therefore more closely approximates the challenge faced by retinal prostheses.

We targeted BT-RGCs owing to the fact that the intrinsic properties of BT-RGCs in the cat are conserved in rat (c.f., A-type RGCs) and likely also in other species [6]. Moreover, in primate retina, most RGCs exhibit brisk-transient or brisk-sustained responses [12]. The BT-RGCs in cat retina therefore provide a relevant model for the study of prosthetic stimulation with reasonable prospects for extrapolation of results to conditions comparable with clinical applications.

V. Conclusion

We quantified the efficacy of electrical stimulation of BT-RGCs using stimulus sequences designed to resemble normal visual responses. Our results demonstrate that stimulus efficacy remains high under such conditions. This suggests that reduced efficacy for electrical stimulation at high frequency, as reported in some previous studies, may not necessarily pose a significant challenge to retinal implants under conditions likely to be encountered in use by an implant wearer.

VI. Acknowledgments

The authors are indebted to Craig Savage who produced the visual stimulus sequences, Brendan O'Brien for expert advice regarding patch-clamp recordings, and to Bill Levick, Ted Maddess, Nicholas Price and Adam Morris for helpful discussion of the analysis.

References

[1] S. I. Fried, H. A. Hsueh, and F. S. Werblin, "A method for generating precise temporal patterns of retinal spiking using prosthetic stimulation," *J. Neurophysiol.*, vol. 95, no. 2, pp. 970–978, 2006.

[2] C. Sekirnjak, P. Hottowy, A. Sher, W. Dabrowski, A. M. Litke, and E. J. Chichilnisky, "Electrical stimulation of mammalian retinal ganglion cells with multielectrode arrays," *J. Neurophysiol.*, vol. 95, no. 6, pp. 3311–3327, 2006.

[3] A. K. Ahuja, M. R. Behrend, M. Kuroda, M. S. Humayun, and J. D. Weiland, "An in vitro model of a retinal prosthesis," *IEEE Trans. Biomed. Eng.*, vol. 55, no. 6, pp. 1744–1753, 2008.

[4] C. Cai, Q. Ren, N. J. Desai, J. F. Rizzo, III, and S. I. Fried, "Response variability to high rates of electric stimulation in retinal ganglion cells," *J. Neurophysiol.*, vol. 106, no. 1, pp. 153–162, 2011.

[5] S. L. Cloherty, R. C. S. Wong, A. E. Hadjinicolaou, H. Meffin, M. R. Ibbotson, and B. J. O'Brien, "Epiretinal electrical stimulation and the inner limiting membrane in rat retina," in *Proc. 34th Annu. Int. Conf. IEEE Eng. Med. Biol. Soc.*, San Diego, CA, 2012, pp. 2989–2992.

[6] R. C. S. Wong, S. L. Cloherty, M. R. Ibbotson, and B. J. O'Brien, "Intrinsic physiological properties of rat retinal ganglion cells with a comparative analysis," *J. Neurophysiol.*, vol. 108, no. 7, pp. 2008–2023, 2012.

[7] A. E. Hadjinicolaou, R. T. Leung, D. J. Garrett, K. Ganesan, K. Fox, D. A. X. Nayagam, M. N. Shivdasani, H. Meffin, M. R. Ibbotson, S. Prawer, and B. J. O'Brien, "Electrical stimulation of retinal ganglion cells with diamond and the development of an all diamond retinal prosthesis," *Biomaterials*, vol. 33, no. 24, pp. 5812–5820, 2012.

[8] W. R. Levick, B. G. Cleland, and M. W. Dubin, "Lateral geniculate neurons of the cat: Retinal inputs and physiology," *Invest. Ophthalmol.*, vol. 11, pp. 302–311, 1972.

[9] W. Bair, E. Zohary, and W. Newsome, "Correlated firing in macaque visual area MT: Time scales and relationship to behavior," *J. Neuroci.*, vol. 21, no. 5, pp. 1676–1697, 2001.

[10] B. G. Cleland, W. R. Levick, and H. Wassel, "Physiological identification of a morphological class of cat retinal ganglion cells," *J. Physiol. (Lond.)*, vol. 248, no. 1, pp. 151–171, 1975.

[11] M. R. Ibbotson, N. A. Crowder, S. L. Cloherty, N. S. C. Price, and M. J. Mustari, "Saccadic modulation of neural responses: Possible roles in saccadic suppression, enhancement, and time compression," *J. Neurosci.*, vol. 28, no. 43, pp. 10 952–10 960, 2008.

[12] R. H. Masland and P. R. Martin, "The unsolved mystery of vision," *Curr. Biol.*, vol. 17, no. 15, pp. R577–R582, 2007.